



## Comparative study of physico-chemical, mineralogical and morphological characteristics of clay from Niger-Maradi: application to the synthesis of ZSM-5 aluminosilicate catalysts

A. I. Abdourahamane<sup>1</sup>, S. Gueu<sup>1\*</sup>, M. Abdou Salam<sup>2</sup>, H. Kone<sup>3</sup>, K. B. Yao<sup>1</sup>

<sup>1</sup> Laboratoire des Procédés Industriels de Synthèse, de l'Environnement et des Energies Nouvelles (LAPISEN), Institut National Polytechnique Felix Houphouët Boigny (INP-HB), Yamoussoukro-BP : 1093, Côte D'Ivoire.

<sup>2</sup> Laboratoire Matériaux, Eaux et Environnement (LAMEE), Université Abdou Moumouni (UAM)- Faculté des Sciences et Techniques (FAST), BP :10896/237, Niger-Niamey

<sup>3</sup>Département des Sciences et Technologies, Université Alassane Ouattara de Bouaké, BP V18 Bouaké 01, Côte d'Ivoire

\*Corresponding author, [gueu05@yahoo.fr](mailto:gueu05@yahoo.fr)

Received 25 July 2022,  
Revised 18 Sept 2022,  
Accepted 19 Sept 2022

### Keywords

- ✓ Raw Clay,
- ✓ Mineral Clay,
- ✓ Characterization,
- ✓ ZSM-5,
- ✓ Synthesis

[Gueu05@yahoo.fr](mailto:Gueu05@yahoo.fr)  
[horosebastien@yahoo.fr](mailto:horosebastien@yahoo.fr)  
Phone: +2250757469812;  
+2250576838511.

### Abstract

The general objective of this work is to characterize a raw clay here named D<sub>1</sub>, from Niger-Maradi, and its clay fraction (named D<sub>2</sub>) in order to detect whether their physico-chemical, mineralogical and morphological characteristics allow them to be used as a structuring support in the synthesis of ZSM-5 aluminosilicate catalysts. Seven (7) analyses were performed on these clays: X-ray Diffraction (XRD), X-ray Fluorescence (XRF), Fourier Transform Infrared Spectroscopy (FT-IR), Cation Exchange Capacity (CEC), Loss on Ignition (LOI), Brunauer, Emmet and Teller Analysis (BET) and Scanning Electron Microscopy (SEM). From these analyses, it appears that D<sub>1</sub> is a mesoporous aluminosilicate material which contains mainly kaolinite, illite, smectite, chlorite and impurities (carbonates, quartz etc). The other one, D<sub>2</sub> is also a mesoporous aluminosilicate material, but with almost no impurities and containing the same clay minerals in the proportions of 81.8% kaolinite, 14.2% illite and 4% of an irregular clay mineral smectite\chlorite; i.e. 96% non-swelling clays (kaolinite and illite) and 4% swelling clays (smectite).

### 1. Introduction

Zeolite catalysts, Zeolite Socony Mobil-Five (ZSM-5), have over the years become the most widely used catalytic materials in the refining industry due to their high acidity and good shape selectivity [1], [2]. They are used in several refining processes including oligomerization [3–8] and catalytic cracking [9–17]. Catalytic cracking is an operation which consists in fragmenting on an acid catalyst at a temperature close to 500°C and at low pressure, hydrocarbons with high molecular weight into hydrocarbons with lower molecular weight [2].

ZSM-5 catalysts can be synthesized from industrial materials such as Tetrapropylammonium (TPA), industrial silica (LUDOX HS-40) and aluminum isopropoxide where they respectively play the role of matrix, additive which provide the hardness to the catalysts and give them reaction sites [18]. Due to TPA's toxic and polluting nature during the synthesis of ZSM-5 catalysts and its high cost, researchers have turned to a much more economical and ecological alternative by using clay minerals [19]. Thus,

researchers such as Pan and *al*, 2017 [20]; Xing and *al*, 2017 [21]; Nanzhe and *al*, 2019 [22]; Yue and *al*, 2020 [23] and Wu and *al*, 2020 [24]; have used kaolinite, attapulgite, illite, rectorite and palygorskite, respectively, to synthesize the ZSM-5 aluminosilicate zeolite catalysts. The synthesis of these catalysts is generally carried out by two ways: the dry way which does not use solvent [25–27] and the hydrothermal way which uses solvent in the experimental protocol [20, 22, 28]. The hydrothermal way is still the most suitable for the synthesis of ZSM-5 catalysts, as the solvent is required for proper crystallization of ZSM-5 zeolite [24].

The need for refining catalysts in Niger and Nigeria is increasing with the planned expansion of the Refining Society of Zinder (SORAZ) in Niger and with the commissioning of the world's largest refinery (650,000 barrels/day), DANGOTE REFINERY, in Nigeria. However, Niger has a great potential in clay materials whose use is generally limited to the construction of houses and in pottery [29–32]. The synthesis of these types of catalysts, ZSM-5, based on clay minerals from Niger could be interesting to these companies.

The main objective of this work was to characterize clays from Niger-Maradi (a raw clay and its fine fraction) in order to discuss the possibility of their use as matrix of ZSM-5 aluminosilicate catalysts.

## 2. Methodology:

### 2.1 Sampling:

The raw clay noted D<sub>1</sub> which is the subject of the present study was collected in Niger in the region of Maradi [figure 1](#) more precisely in the locality of Djirataoua (GPS coordinates: Depth 3m; Latitude N 13°24'39,6"; Longitude E 7°08'41'6").



**Figure 1:** Sampling site location.

### 2.2 Preparation of the purified clay:

The purified clay named D<sub>2</sub> was obtained from raw clay D<sub>1</sub> following the procedure proposed by Medard Thiry et al [33, 34]. First, the raw clay D<sub>1</sub> underwent the decarbonation and destruction operations of the organic matter respectively with hydrochloric acid HCl and hydrogen peroxide H<sub>2</sub>O<sub>2</sub> at 10%. The mixture of water D<sub>1</sub> and raw clay was gently stirred during the treatment to accelerate the release of clay minerals. If the water in the beaker is quite cloudy, the water is collected without residue from the bottom. However, if the water remained clear, it is necessary to treat with ultrasound. The

rinsing is done with the centrifugator and its aim is to eliminate dissolved impurities in the water in order to promote a better deflocculation of the clay minerals. To eliminate these impurities, it is necessary to put the mixture water and D<sub>1</sub> into the centrifugator by proceeding as follows: centrifuge at 3000 trs/mn during 10 mn, then, to repeat the operation until obtaining a turbid solution. The clay minerals were only extract from cloudy solution. It was carried out by means of centrifugation by to the following procedure:

- add few drops of ammonia to accelerate deflocculation;
- start the centrifugation at 1000 rpm during 1 mn 06 s;
- stop the machine and remove the supernatant.

Finally, the clay mineral was put in a porcelain crucible and dried at 60°C. This clay minerals sample obtained was noted D<sub>2</sub>.

## **2.3 Analysis Methods:**

### **2.3.1 X-Ray Diffraction (XRD):**

X-ray Diffraction (XRD) was performed on raw clay D<sub>1</sub> and on the Clay Fraction D<sub>2</sub>. The XRD analysis on sample D<sub>1</sub> was performed with an ANCHOR SCAN version "1.0" Diffractogram at Ahmed Bello University (ABU) in the Federal Republic of Nigeria. The scan is from 5.02 to 75.97° in 0.02 s steps with a duration of 29.07 s; Cu anticathode; 45 kV-40mA.

XRD analysis on the clay fraction D<sub>2</sub> occurred on an oriented slide. For this purpose, pillboxes of 30ml capacity are shaken by hand in order to suspend 30 ml volume of the clay minerals, then left to stand for 50 minutes. After decantation, the upper part of the suspension is carefully taken with a pipette on a height of 02 cm. The collected clay solution is air-dried on a glass slide. Once dried, the slide is analyzed by XRD; using the Bruker D8 ADVANCE diffractometer and is then placed in an ethylene glycol saturated atmosphere for 12 hours.

The slide is again analyzed by XRD and then heated in an oven at 550 °C for 2 hours and analyzed again by XRD. The identification and quantification of minerals were performed using the FITYK software. The intensity correction factors of Thorez (1976) were used for the quantification of clay minerals. The extraction of D<sub>2</sub> and its analysis by XRD were carried out at the PETROCI Analysis and Research Center in the Republic of Ivory Coast.

### **2.3.2 X-Ray Fluorescence (XRF):**

X-ray fluorescence (FRX) was carried out using a THERMO-SCIENTIFIC instrument at the Geology Laboratory of the African Centre of Excellence in Mining and Mining Environment (CEA-MEM) of the INP-HB of Yamoussoukro (Ivory Coast) to determine samples D<sub>1</sub> and D<sub>2</sub> elemental mineralogical composition. Measurements in "MINING" mode, in the 2θ range for 120 min, were performed on an accessory equipped with a RFID (Radio Frequency Identification) chip allowing the analyzer to detect it automatically in order to convert it into a benchtop analyzer. The data transfer was done directly on computer thanks to a powerful reader called Niton XL3t coupled with a NDF software.

### **2.3.3 Infrared Spectroscopy (IR):**

Infrared spectroscopy (FT-IR) was carried out in ATR (Attenuated Total Reflectance) mode on D<sub>1</sub> and D<sub>2</sub>, at the Spectral Laboratory of the University of Kaduna, Federal Republic of Nigeria, with a Bruker Alpha Fourier Transform Spectrometer, brand SHIMADZU, equipped with a diamond crystal in the wavelength range from 400 cm<sup>-1</sup> to 4000 cm<sup>-1</sup>.

### 2.3.4. Cation Exchange Capacity (CEC):

Clays are characterized by a Cationic Exchange Capacity (CEC), which is defined as the number of monovalent cations that can be substituted for the compensating cations present in their interfoliar spaces, to balance the electrical charge of 100 g of calcined clay. The CEC of clay minerals is expressed in meq/100g. Among the existing methods for the determination of the CEC, those of Mantin and Glaeser [34] using cobalthexamine was chosen. This method allows to determine in the supernatant, the concentration of cobalthexamine not retained by the clay. Based on the colorimetric measurement, by means of a visible-UV spectrometer.

In the present work, a mixture of 100 mg of clay ( $D_1$  or  $D_2$ ) and 25 ml of the cobalthexamine solution of initial concentration  $C_i = 5.10^{-3}$  mol/l is maintained under a stirring for 3h. After centrifugation, the supernatant is recovered and the final concentration  $C_f$  of the cobalthexamine solution is measured from the absorbance recorded at 476 nm with a UV/Vis/NIR spectrophotometer using the Beer-Lambert law. The amount of cobalthexamine retained per 100 mg of raw clay  $D_1$  (or clay fraction  $D_2$ ) is determined by the difference of the concentration  $C_i$  and  $C_f$ .

### 2.3.5. Loss On Ignition (LOI):

The loss on ignition or loss in weight expressed in percentage (%) is the weight of a sample after calcination at 1100°C, compared to the initial weight of the sample. It allows to know the quantity of the products likely decomposed or volatilized during the calcination. The loss on ignition of clay samples was measured by introducing a mass  $P$  of this clay in a porcelain crucible previously tared. The crucible was placed in an oven, with a gradual increase of the temperature to 1000°C for 1h. The crucible is then placed in a desiccator to cool it and weighed; the mass obtained was  $P'$  [35]. The value of the loss on ignition is given by the following formula:

$$PAF = \frac{P - P'}{P} \times 100 \quad \text{Eqn. 1}$$

### 2.3.6 Brunauer-Emmet-Teller (BET) analysis:

The physical characteristics of  $D_1$  and  $D_2$  were obtained through Brunauer, Emmet and Teller (BET) analysis which was carried out using an apparatus called QUANTACHROME-NOVAWIN version 11.03 at the University of Kaduna, Federal Republic of Nigeria. For this purpose; 0, 12 g of the sample was taken, which sample was subjected to adsorption and desorption of  $N_2$  at 77.350°K for 3 hours.

### 2.3.7 Scanning Electron Microscopy (SEM):

Scanning Electron Microscope (SEM) observation was performed on  $D_1$  and  $D_2$  to visualize the morphology of these samples.

## 3. Results and discussion:

### 3.1 X-Ray Diffraction (XRD):

The result of the raw clay  $D_1$  X-ray diffraction (XRD) analysis is shown in the following Figure 2. In Figure 2 above, peaks are observed around: 9° (2θ) characteristic of Illite [(K, H<sub>3</sub>O) (Al, Mg, Fe)<sub>2</sub> (Si, Al)<sub>4</sub> O<sub>10</sub>((OH)<sub>2</sub>, (H<sub>2</sub>O))] [36, 37], 12° (2θ) characteristic of Kaolinite [(Al<sub>2</sub>Si<sub>2</sub>O<sub>9</sub>H<sub>4</sub>)] [38], 21° (2θ) and 26° (2θ) characteristic of quartz [Si<sub>3</sub>O<sub>6</sub>], finally, 22° (2θ) and 28° (2θ) characteristic of Feldspar [KAlSi<sub>3</sub>O<sub>8</sub>] [39].  $D_1$  sample contains; besides clay minerals such as illite, kaolinite and feldspar other elements considered as non-clay including; free quartz. The presence of free quartz in the clay is undesirable for its use in the ZSM-5 catalyst synthesis according to the work of Xing and al [21], Pan

and *al* [20], and Liu and *al* [40]. X-ray diffractogram of the fine fraction D<sub>2</sub> is presented in figure 3 below.

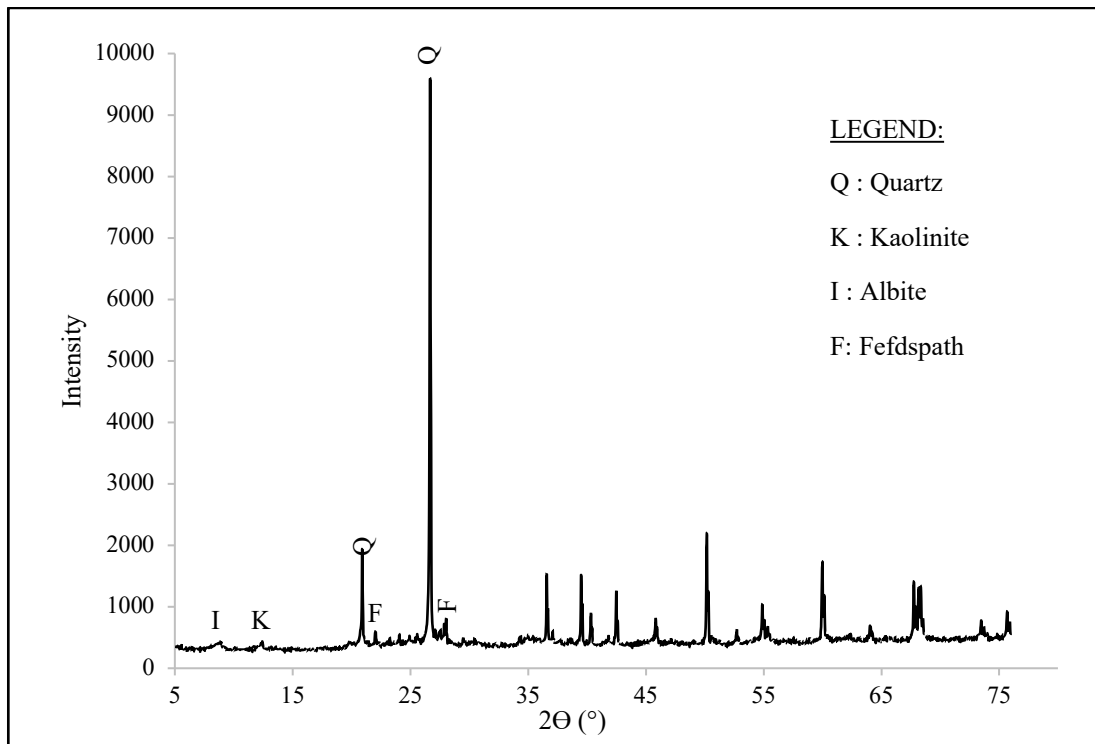


**Figure 2:** Raw clay D<sub>1</sub> X-ray diffractogram

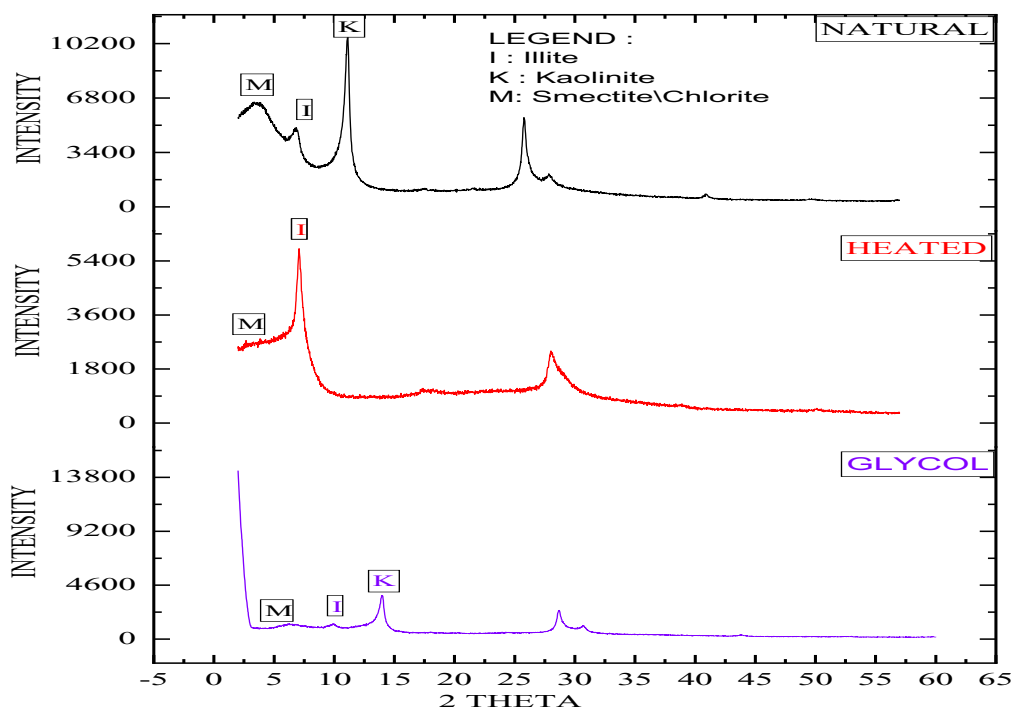


**Figure 3:** Natural clay fraction D<sub>2</sub> X-ray diffractogram, treated with ethylene glycol then heated to 550°C.

Figure 3 above shows the results of the natural D<sub>2</sub> clay fraction XRD analysis, treated with ethylene glycol and heated to 550°C. The spectra analysis using the clay mineral identification and quantification software, FITYK, showed characteristic pics of kaolinite (K), illite (I) and smectite

(smectite\chlorite: M) [29]. It should be noted that elements such as feldspar and quartz are no longer present in the clay fraction (figure 2). This indicates that the purification operations employed here were well carried out. The quantification of the clay minerals present in the clay fraction shows a large predominance of kaolinite with 81.8%. The illite content was estimated at 14% while that of smectite is 4%. This mineralogical composition indicates that this Niger-Maradi clay is a mixed clay, i.e. it contains 96% non-swelling clays (kaolinite and illite) and 4% swelling clays (smectite). These results are similar to those obtained by O.D.M Abdoulaye and *al*, 2019 during their work on the mineralogical and morphological characterization of a clay from Niger-Tahoua [31]. These results are also similar to those of M.A Maman *et al*, 2017 [41] and M. Gourouza *et al*, 2013 [29]. In view of the use of clay made by the previously mentioned authors, Niger-Maradi D<sub>2</sub> clay sample can also be used for the synthesis of the aluminosilicate catalyst ZSM-5.

### 3.2 Fluorescence des Rayons-X (FRX) :

Elemental chemical analysis by X-ray fluorescence (XRF) was performed on D<sub>1</sub> and D<sub>2</sub>. The results of this analysis indicate the predominance of silica and alumina in D<sub>1</sub> and D<sub>2</sub>, according to Table 1 below:

**Table 1:** Chemical composition and SiO<sub>2</sub>/Al<sub>2</sub>O<sub>3</sub> ratio of D<sub>1</sub> and D<sub>2</sub>.

Oxides (%)	Samples	
	D <sub>1</sub>	D <sub>2</sub>
SiO <sub>2</sub>	58.851	42.888
Al <sub>2</sub> O <sub>3</sub>	14.515	20.096
Fe <sub>2</sub> O <sub>3</sub>	8.294	12.354
MgO	3.27	2.366
P <sub>2</sub> O <sub>5</sub>	0.8877	0.3305
SO <sub>3</sub>	0.0784	0.1178
TiO <sub>2</sub>	0.8425	0.8954
MnO	0.7536	0.2161
CaO	0.8793	1.4001
K <sub>2</sub> O	2.1432	0.9424
Na <sub>2</sub> O	1.8770	0.607
ZrO <sub>2</sub>	0.1661	0.0129
SrO	0.156	0.2769
Others	7.2862	17.4969
SiO <sub>2</sub> /Al <sub>2</sub> O <sub>3</sub>	4.054	2.134

These results show that, for the D<sub>1</sub> case, the percentage of silica and alumina is very high, i.e. SiO<sub>2</sub>/Al<sub>2</sub>O<sub>3</sub> ratio equal to 4.054. This is significantly higher than the classical SiO<sub>2</sub>/Al<sub>2</sub>O<sub>3</sub> ratio of kaolinite which is lower than 2 [42]. This remarkable difference indicates the probable presence of free quartz in D<sub>1</sub> in great proportion [43], hence the need to proceed to the extraction of the clay fraction D<sub>2</sub>. In the clay fraction D<sub>2</sub>, a decrease in SiO<sub>2</sub> content and an increase in Al<sub>2</sub>O<sub>3</sub> content were observed, resulting in a SiO<sub>2</sub>/Al<sub>2</sub>O<sub>3</sub> ratio equal to 2.134, which is slightly higher than that of kaolinite [42]. This could be explained by the purification that D<sub>1</sub> sample underwent. There is also a significant increase in the content of other oxides such as iron (Fe<sub>2</sub>O<sub>3</sub>), calcium (CaO) and titanium (TiO<sub>2</sub>).

In addition, this analysis shows that the D<sub>2</sub> sample contains almost no metals (trace) such as vanadium and nickel. However, a high concentration of these metals in natural clay minerals could negatively affect the performance of a catalyst, according to E. A. Emam [39]. Metals such as vanadium and nickel also cause catalysts poisoning and eventually cause their deactivation [44].

### 3.3 Infrared Spectroscopy (IR):

Fourier Transform Spectrometry (IR) was performed on D<sub>1</sub> and D<sub>2</sub> samples in order to complete the X-ray diffraction. This analysis allowed to highlight the nature of the chemical bonds as well as the nature of the atoms involved in these bonds; almost unobservable with the X-ray diffraction. The following figure 4 and figure 5 give the IR spectrum of D<sub>1</sub> and D<sub>2</sub> respectively.

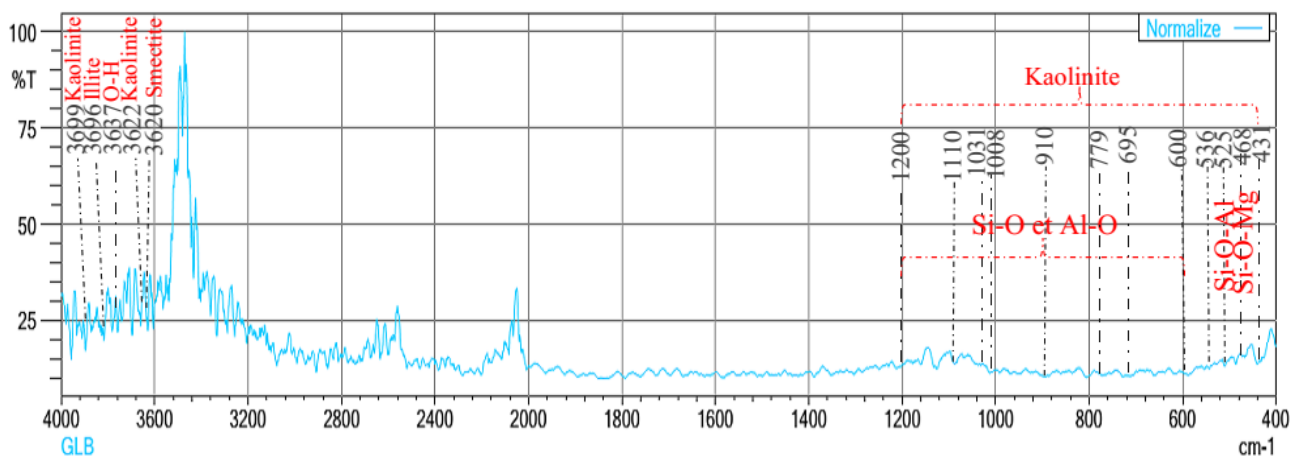


Figure 4: IR spectrum of D<sub>1</sub> sample

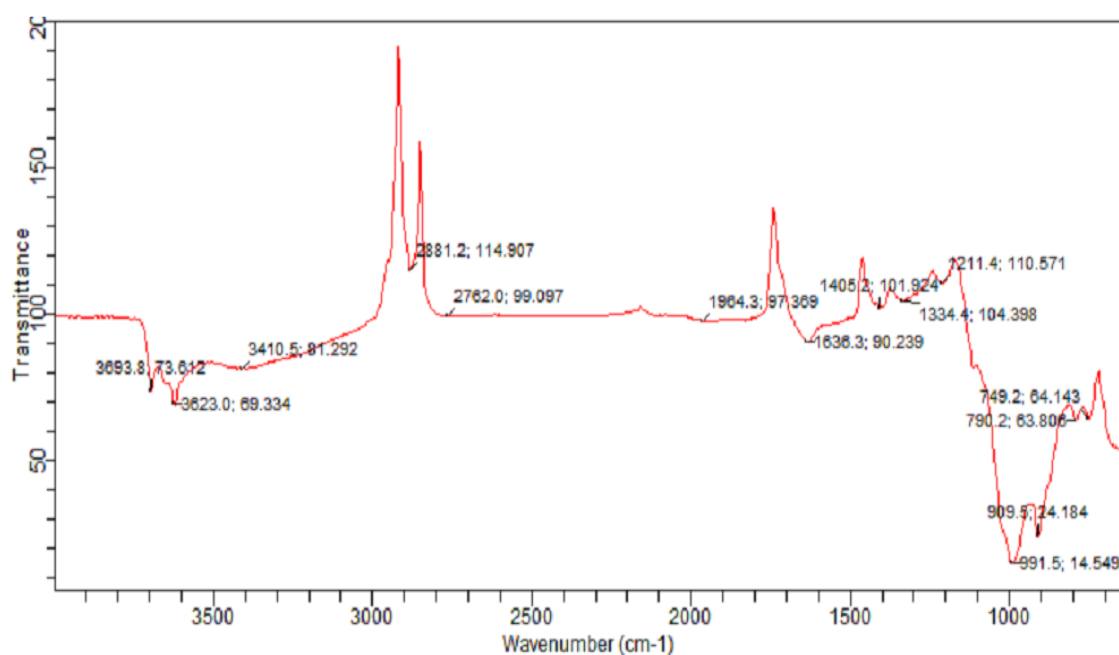


Figure 5: IR spectrum of D<sub>2</sub> sample

The observable bands between 600 and 1200  $\text{cm}^{-1}$ , on figure 4, indicate the presence of aluminosilicates in the D<sub>1</sub> sample, thus on the Si-O and Al-O interatomic bonds [45]. According to O. Bouras, the bands between 468 and 525  $\text{cm}^{-1}$  are those of the vibrations of the formation of Si-O-Mg and Si-O-Al [46]. The bands at 3699, 3622, 1110, 1031, 1008, 910  $\text{cm}^{-1}$ , are those of kaolinite [47, 48]. The characteristic vibrational bands of quartz are observed at 779 and 695  $\text{cm}^{-1}$  [48]. Indeed, other vibrational bands of Si-O formation are observed around 1017 and near 1019  $\text{cm}^{-1}$  and a hydroxyl formation vibrational band around 1637  $\text{cm}^{-1}$  [43, 49].

It can be seen on the IR spectrum of D<sub>2</sub> (figure-5) that the characteristic vibrational bands of quartz (779 and 695  $\text{cm}^{-1}$ ), are no longer observable. This can be explained by the purification of the D<sub>2</sub> sample

which allowed the removal of quartz crystals, organic matter and carbonates. The observable bands around 468 and 525  $\text{cm}^{-1}$  characteristics of Si-O-Mg and Si-O-Al [46] formation vibrations are replaced by bands around 749.2 and 790.2  $\text{cm}^{-1}$  [50]. The latter are assigned to the vibrations of the elongation of Si-O-Al bonds and hydroxyls perpendicular to the surface (translational O-H) [45]. The characteristic bands of kaolinite are observable between 909.5 and 1211.4  $\text{cm}^{-1}$  on the D<sub>2</sub> IR spectrum. Other adsorption bands characteristic of phyllosilicates (illite, smectite and chlorite) are observed around 3623 and 3693.8  $\text{cm}^{-1}$ . These results of the IR analysis are in perfect agreement with the results of the X-ray diffraction in that they reveal that D<sub>1</sub> sample contains, in addition to quartz crystals, phyllosilicate clay minerals such as kaolinite, illite, smectite and chlorite. As for D<sub>2</sub> sample, it contains only clay minerals (kaolinite, illite, smectite and chlorite).

Yet, several authors have used phyllosilicate clay minerals to synthesize ZSM-5 zeolite. Yue and *al*, 2018 [19] used, in addition to diatomite, rectorite, which is a two-phyllosilicate clay mineral (smectite and mica) to synthesize ZSM-5. Xing-Yang and *al*, 2017 [21], used attapulgite which is a phyllosilicate mineral to synthesize the aluminosilicate catalyst ZSM-5. Liu and *al*, 2019 [22], also used illite which is a non-swelling phyllosilicate clay mineral to synthesize ZSM-5.

In the same way Wu and *al* 2020 [24] also used palygorskite, which is a phyllosilicate clay mineral, to synthesize the ZSM-5 catalyst. Yue and *al*, 2020 [19] used alleverdite, which is a regular clay mineral with two phyllosilicates (smectite and mica), to synthesize the zeolitic aluminosilicate catalyst ZSM-5 as well. As the purified clay, D<sub>2</sub> contains clay minerals (kaolinite, illite, smectite and chlorite). It could be used for the synthesis of zeolitic aluminosilicate catalysts ZSM-5.

### **3.4 Cation Exchange Capacity (CEC):**

The CEC value of D<sub>1</sub> found is 22.8 meq/100g while that of D<sub>2</sub> is 40 meq/100g. It can be seen that both CEC values found exceed the range of CEC value of standard kaolinite, which is 1-3 [43]. They are between 10-40 which is the range of CEC value of standard illite [4]. This confirms the simultaneous presence of clay minerals such as kaolinite and illite in D<sub>1</sub> and D<sub>2</sub>, hence the mixed character of D<sub>1</sub> and D<sub>2</sub>. It is also noted that the CEC value of D<sub>2</sub> is higher than the CEC value of D<sub>1</sub>. This is probably due to the presence of impurities (carbonates, quartz, hematite etc) in D<sub>1</sub> [37, 51].

Indeed, the knowledge of these CEC values (22.8 meq/100g for D<sub>1</sub> and 40 meq/100g for D<sub>2</sub>) indicates the presence of clay minerals such as kaolinite, illite etc. in the samples (D<sub>1</sub> and D<sub>2</sub>). According to Abdoulaye and *al* [31], Mahmoudi and *al* and Murray [41, 52]; the use of these minerals as a catalytic support is very advantageous, since they might guarantee the performance of catalysts.

### **3.5 Loss on ignition (LOI):**

The loss on ignition value of D<sub>1</sub> obtained is 6.30%, which is an intermediate value and that of D<sub>2</sub> obtained is 18%. The latter may be related to the decrease in silicate and carbonate mineral contents during purification. This decrease could be due to the loss of adsorbed water and dehydroxylation of phyllosilicates [43]. This confirms XRF analysis which also shows a decrease in the proportions of silicate minerals ( $\text{SiO}_2$ ) during the transition from D<sub>1</sub> to D<sub>2</sub>.

### **3.6 Brunauer, Emmet and Teller (BET) analysis:**

This analysis allowed us to study the physical characteristics of D<sub>1</sub> and D<sub>2</sub> samples, by the N<sub>2</sub> adsorption-desorption isotherms, i.e. specific surface area (SS), pore volume (VP) and pore diameter (DP). The results of this analysis are compiled in Table 2.

**Table 2:** Specific surface area (SS), pore volume (VP) and pore diameter (DP) data of D<sub>1</sub> and D<sub>2</sub>.

	Surface area (m <sup>2</sup> /g)	Pore volume (cm <sup>3</sup> /g)	Pore diameter (nm)
D <sub>1</sub>	446.5	0.2201	2.128
D <sub>2</sub>	256.3	0.1267	2.100

Table 2 above shows specific surface, pore volume and pore diameter results of D<sub>1</sub> and D<sub>2</sub>. The BET specific surface area (SS) of D<sub>1</sub> decreased when switching from D<sub>1</sub> to D<sub>2</sub> (after treatment). It decreased from 446.5 to 256.3 m<sup>2</sup>/g. The pore diameter decreased from 2.128 to 2.100 nm; the pore volume was also reduced from 0.2201 to 0.1267 cm<sup>3</sup>/g. In view of these results, we can state that sample D<sub>1</sub> and D<sub>2</sub> are all mesoporous, if we limit to the classification proposed by Dubinin adopted by the International Union of Pure and Applied Chemistry (IUPAC) [53]. In addition, D<sub>1</sub> and D<sub>2</sub> have a good specific surface area for adsorption, according to the European patent for the ZSM-5 synthesis, as it is between 100 and 550 nm [54]. The mesoporous morphology, according to S. Moon et al, 2018, is suitable for ZSM-5 aluminosilicate catalysts analysis [5].

### 3.7 Scanning Electron Microscopy (SEM):

Scanning electron microscopy allows, to observe not only the texture of clay samples, but also to characterize the mineralogical assemblages. Images obtained from D<sub>1</sub> (a) and D<sub>2</sub> (b) by SEM with magnifications of 100μm are shown in the following Figure 6.

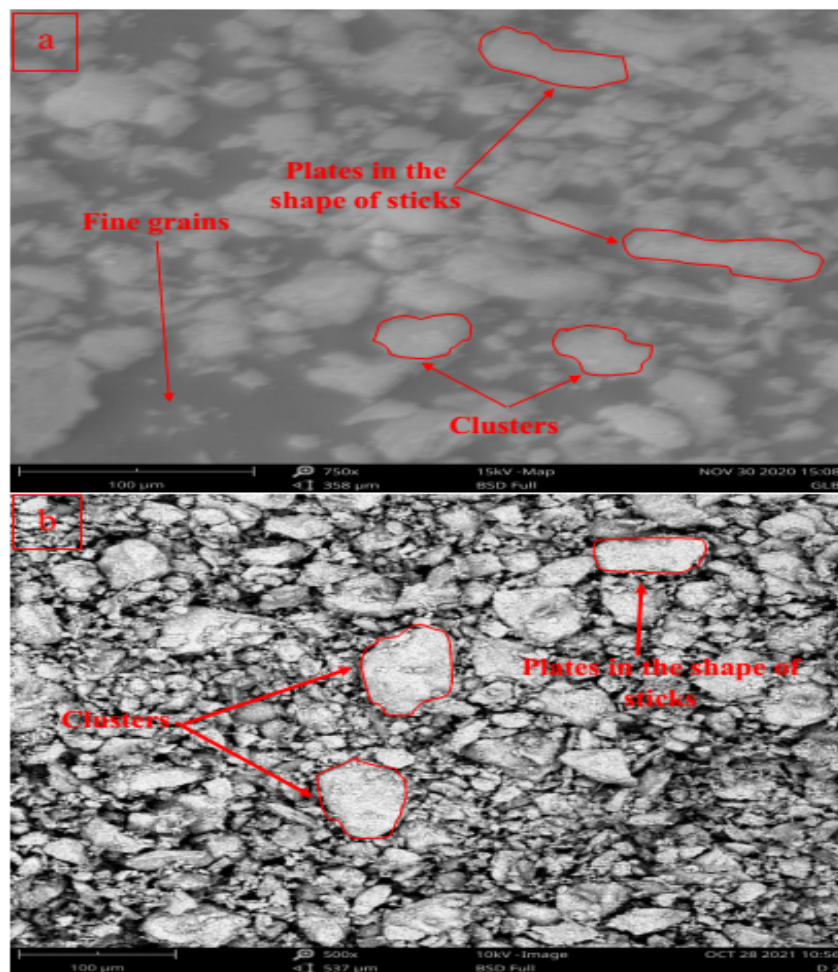


**Figure 6:** D<sub>1</sub> (a) and D<sub>2</sub> (b) at 100μm magnifications Scanning Electron Microscopy (SEM) images.

The images in Figure 6 above show clay particles with irregularly contoured rod-like platelets and clusters in the D<sub>1</sub> (a) and D<sub>2</sub> (b) images. These morphologies, as observed by A. Qlihaa [43], are characteristic of kaolinite, illite and other poorly crystallized clay minerals such as smectite and chlorite [43]. This shows that D<sub>1</sub> and D<sub>2</sub> samples contain kaolinite, illite, smectite and chlorite. It can be seen that sample D<sub>2</sub> has a higher concentration, compared to sample D<sub>1</sub>, of clay particles in the form of rod-like platelets and clusters. Thus, sample D<sub>2</sub> contains more clay minerals than D<sub>1</sub>. The clusters clearly observable in the image of D<sub>1</sub> (a) reflect the presence of carbonates and the small grains observable in D<sub>1</sub> also reflect the presence of quartz [55] in the D<sub>1</sub> sample. These results are in agreement with the results of the XRD and XRF analysis.

## Conclusion

Experimental techniques such as X-ray Diffraction (XRD), X-ray Fluorescence (XRF), Fourier Transform Infrared Spectroscopy (FT-IR), Cation Exchange Capacity (CEC), Loss on Ignition (LOI), Brunauer, Emmet and Teller Analysis (BET) and Scanning Electron Microscopy (SEM) used in the present work of characterization of the raw clay D<sub>1</sub> from Niger-Maradi and its clay fraction D<sub>2</sub>; allowed to highlight the physicochemical, mineralogical and morphological aspects of D<sub>1</sub> and D<sub>2</sub> samples. Thus, it was established that the sample D<sub>1</sub> is a mesoporous aluminosilicate material which contains essentially clay minerals, in the form of clusters and fine aggregates, such as kaolinite, illite, smectite, chlorite and impurities (carbonates, quartz etc). D<sub>2</sub> is also a mesoporous aluminosilicate material, but with almost no impurities and contains the same clay minerals in the form of clusters and fine aggregates, in the proportions of 81,8% of kaolinite, 14,2% of illite and 4% of an irregular clay mineral smectite\chlorite. D<sub>1</sub> has a SiO<sub>2</sub>\Al<sub>2</sub>O<sub>3</sub> ratio of 4.054% while that of the clay fraction D<sub>2</sub> is 2.134%. The CEC of D<sub>1</sub> and D<sub>2</sub> are 22.8 meq/100g and 40 meq/100g respectively. The loss on ignition of the sample D<sub>1</sub> and D<sub>2</sub> are respectively 6.30% and 18%. D<sub>1</sub> has a specific surface area (SS) of 446.5 m<sup>2</sup>/g, a pore diameter (PD) of 2.128 nm and a micropore volume (MPV) of 0.2201 cm<sup>3</sup>/g while D<sub>2</sub> has a specific surface area (SS) of 256.3 m<sup>2</sup>/g, a pore diameter (PD) of 2.100 nm and a micropore volume (MPV) of 0.1267 cm<sup>3</sup>/g. In relation to the results previously presented, we can affirm that the samples of raw clay D<sub>1</sub> and of the fine fraction D<sub>2</sub> of Niger-Maradi have the physico-chemical, mineralogical and morphological characteristics required to be used in the synthesis of ZSM-5 aluminosilicate zeolite catalysts.

## Acknowledgement

The authors thank Mr David English PhD student, for reading and correcting the manuscript, thus contributing to improve the paper quality.

**Disclosure statement:** *Conflict of Interest:* The authors declare that there is no potential conflict of interest was reported by the author(s)

*Compliance with Ethical Standards:* This article does not contain any studies involving human or animal subjects.

## References

- [1] T. F. Degnan, G. K. Chitnis, P. H. Schipper, History of ZSM-5 fluid catalytic cracking additive development at Mobil, *Microporous Mesoporous Mater.*, 35-36 (2022) 245-252, [doi: 10.1016/S1387-1811\(99\)00225-5](https://doi.org/10.1016/S1387-1811(99)00225-5).

- [2] W. Luo, X. Yang, Z. Wang, W. Huang, J. Chen, W. Jiang, L. Wang, X. Cheng, Y. Deng, D. Zhao, Synthesis of ZSM-5 aggregates made of zeolite nanocrystals through a simple solvent-free method, *Microporous Mesoporous Mater.*, 243 (2017) 112-118, [doi: 10.1016/j.micromeso.2017.01.040](https://doi.org/10.1016/j.micromeso.2017.01.040)
- [3] A. de Klerk, Oligomerization of 1-Hexene and 1-Octene over Solid Acid Catalysts, *Ind. Eng. Chem. Res.*, 44 (2005) 3887-3893, [doi: 10.1021/ie0487843](https://doi.org/10.1021/ie0487843).
- [4] N. G. Grigor'eva, D. V. Serebrennikov, S. V. Bubennov, B. I. Kutepov, Oligomerization of 1-Pentene on Zeolite Catalysts, *Catal. Ind.*, 12 (2020) 47-55, [doi: 10.1134/S2070050420010079](https://doi.org/10.1134/S2070050420010079).
- [5] S. Moon, H.-J. Chae, M. B. Park, Oligomerization of light olefins over ZSM-5 and beta zeolite catalysts by modifying textural properties, *Appl. Catal. Gen.*, 553 (2018) 15-23, [doi: 10.1016/j.apcata.2018.01.015](https://doi.org/10.1016/j.apcata.2018.01.015).
- [6] C. P. Nicholas, L. Laipert, et S. Prabhakar, Oligomerization of Light Olefins to Gasoline: An Advanced NMR Characterization of Liquid Products, *Ind. Eng. Chem. Res.*, 55 (2016) 9140-9146, [doi: 10.1021/acs.iecr.6b01591](https://doi.org/10.1021/acs.iecr.6b01591).
- [7] W. Monama, E. Mohiuddin, B. Thangaraj, M. M. Mdleleni, D. Key, Oligomerization of lower olefins to fuel range hydrocarbons over texturally enhanced ZSM-5 catalyst, *Catal. Today*, S0920586119300860 (2019), [doi: 10.1016/j.cattod.2019.02.061](https://doi.org/10.1016/j.cattod.2019.02.061).
- [8] G. Bellussi, F. Mizia, V. Calemma, P. Pollesel, R. Millini, Oligomerization of olefins from Light Cracking Naphtha over zeolite-based catalyst for the production of high quality diesel fuel, *Microporous Mesoporous Mater.*, 164 (2012) 127-134, [doi: 10.1016/j.micromeso.2012.07.020](https://doi.org/10.1016/j.micromeso.2012.07.020).
- [9] S. Sukanuma, N. Katada, Innovation of catalytic technology for upgrading of crude oil in petroleum refinery, *Fuel Process. Technol.*, 208 (2020) 106518, [doi: 10.1016/j.fuproc.2020.106518](https://doi.org/10.1016/j.fuproc.2020.106518).
- [10] E. Y. Emori, F. H. Hirashima, C. H. Zandonai, C. A. Ortiz-Bravo, N. R. C. Fernandes-Machado, M. H. N. Olsen-Scaliante, Catalytic cracking of soybean oil using ZSM5 zeolite, *Catal. Today*, 279 (2017) 168-176, [doi: 10.1016/j.cattod.2016.05.052](https://doi.org/10.1016/j.cattod.2016.05.052).
- [11] H. Huang, H. Zhu, S. Zhang, Q. Zhang, C. Li, Effect of silicon to aluminum ratio on the selectivity to propene in methanol conversion over H-ZSM-5 zeolites, *J. Fuel Chem. Technol.*, 47 (2019) 74-82, [doi: 10.1016/S1872-5813\(19\)30005-2](https://doi.org/10.1016/S1872-5813(19)30005-2).
- [12] A. Ishihara, Preparation and reactivity of hierarchical catalysts in catalytic cracking, *Fuel Process. Technol.*, 194 (2019) 106116, [doi: 10.1016/j.fuproc.2019.05.039](https://doi.org/10.1016/j.fuproc.2019.05.039).
- [13] M. Pan, J. Zheng, Y. Liu, W. Ning, H. Tian, R. Li, Construction and practical application of a novel zeolite catalyst for hierarchically cracking of heavy oil, *J. Catal.*, 369 (2019) 72-85, [doi: 10.1016/j.jcat.2018.10.032](https://doi.org/10.1016/j.jcat.2018.10.032).
- [14] M. A. Sanhoob, O. Muraza, E. N. Shafei, T. Yokoi, K.-H. Choi, Steam catalytic cracking of heavy naphtha (C12) to high octane naphtha over B-MFI zeolite, *Appl. Catal. B Environ.*, 210 (2020) 432-443, [doi: 10.1016/j.apcatb.2017.04.001](https://doi.org/10.1016/j.apcatb.2017.04.001).
- [15] A. Talebian-Kiakalaieh, S. Tarighi, Synthesis of hierarchical Y and ZSM-5 zeolites using post-treatment approach to maximize catalytic cracking performance, *J. Ind. Eng. Chem.*, 88 (2020) 167-177, [doi: 10.1016/j.jiec.2020.04.009](https://doi.org/10.1016/j.jiec.2020.04.009).
- [16] Y. Wang, J. Song, N. C. Baxter, G.-T. Kuo, S. Wang, Synthesis of hierarchical ZSM-5 zeolites by solid-state crystallization and their catalytic properties, *J. Catal.*, 349 (2017) 53-65, [doi: 10.1016/j.jcat.2017.03.005](https://doi.org/10.1016/j.jcat.2017.03.005).

- [17] T. Zhao, F. Li, H. Yu, S. Ding, Z. Li, X. Huang, X. Li, X. Wei, Z. Wang, H. Lin, Synthesis of mesoporous ZSM-5 zeolites and catalytic cracking of ethanol and oleic acid into light olefins, *Appl. Catal. Gen.*, 575 (2019) 101-110, [doi: 10.1016/j.apcata.2019.02.011](https://doi.org/10.1016/j.apcata.2019.02.011).
- [18] T. Biligetu, Y. Wang, T. Nishitoba, R. Otomo, S. Park, H. Mochizuki, J. N. Kondo, T. Tatsumi, T. Yokoi, Al distribution and catalytic performance of ZSM-5 zeolites synthesized with various alcohols, *J. Catal.*, 353 (2017) 1-10, [doi: 10.1016/j.jcat.2017.06.026](https://doi.org/10.1016/j.jcat.2017.06.026).
- [19] Y. Yue, Y. Kang, Y. Bai, L. Gu, H. Liu, J. Bao, T. Wang, P. Yuan, H. Zhu, Z. Bai, X. Bao, Seed-assisted, template-free synthesis of ZSM-5 zeolite from natural aluminosilicate minerals, *Appl. Clay Sci.*, 158 (2018) 177-185, [doi: 10.1016/j.clay.2018.03.025](https://doi.org/10.1016/j.clay.2018.03.025).
- [20] F. Pan, X. Lu, T. Wang, Y. Yan, Submicron ZSM-5 synthesized by green and fast route, *Mater. Lett.*, 196 (2017) 245-247, [doi: 10.1016/j.matlet.2017.03.060](https://doi.org/10.1016/j.matlet.2017.03.060).
- [21] L. X. Yang, J. Yao, L. X. Qin, S. L. Ying, Z. D. Yuan, S. L. Bing, Direct Synthesis of Zeolites from a Natural Clay, Attapulgit, *ACS sustainable Chemistry Engineering*, 6 (2017), [doi: 10.1021/acs.suschemeng.7b01001](https://doi.org/10.1021/acs.suschemeng.7b01001).
- [22] Y. Liu, S. Han, D. Guan, S. Chen, Y. Wu, Y. Yang, N. Jiang, Rapid green synthesis of ZSM-5 zeolite from leached illite clay, *Microporous Mesoporous Mater.*, 280 (2019) 324-330, [doi: 10.1016/j.micromeso.2019.02.027](https://doi.org/10.1016/j.micromeso.2019.02.027).
- [23] Y. Yue, Y. Hu, P. Dong, X. Li, H. Liu, J. Bao, T. Wang, X. Bi, H. Zhu, P. Yuan, Z. Bai, X. Bao, Mesoscale depolymerization of natural rectorite mineral via a quasi-solid-phase approach for zeolite synthesis, *Chem. Eng. Sci.*, 220 (2020) 115635, [doi: 10.1016/j.ces.2020.115635](https://doi.org/10.1016/j.ces.2020.115635).
- [24] M. Wu, W. Jiang, J. Jiang, Y. Zou, P. Zhang, P. Mao, Y. Xu, Y. Shi, Synthesis of ZSM-5 zeolites using palygorskite as raw material under solvent-free conditions, *Bull. Mater. Sci.*, 43 (2020) 289, [doi: 10.1007/s12034-020-02263-8](https://doi.org/10.1007/s12034-020-02263-8).
- [25] Y. Wang, H. Duan, Z. Tan, X. Meng, F.-S. Xiao, Illuminating solvent-free synthesis of zeolites, *Dalton Trans*, 49 (2020) 6939-6944, [doi: 10.1039/D0DT00142B](https://doi.org/10.1039/D0DT00142B).
- [26] Y. Ji, Y. Wang, B. Xie, F.-S. Xiao, Zeolite Seeds: Third Type of Structure Directing Agents in the Synthesis of Zeolites, *Comments Inorg. Chem.*, 36 (2016) 1-16, [doi: 10.1080/02603594.2015.1031375](https://doi.org/10.1080/02603594.2015.1031375).
- [27] X. Meng, F. S. Xiao, Green Routes for Synthesis of Zeolites, *Chem. Rev.*, 114 (2014) 1521-1543, [doi: 10.1021/cr4001513](https://doi.org/10.1021/cr4001513).
- [28] L. Zhang, Z. Bao, S. Xia, Q. Lu, K. Walters, Catalytic Pyrolysis of Biomass and Polymer Wastes, *Catalysts*, 8 (2018) 659, [doi: 10.3390/catal8120659](https://doi.org/10.3390/catal8120659).
- [29] M. Gourouza, A. Zanguina, I. Natatou, A. Boos, Characterisation d'une argile mixte du niger characterization of a mixed clay Niger, 1 (2013), 11.
- [30] M. Abdoukader, I. M. S. Souleymane, H. Bouba, A.T. Amadou, G. Zibo, W. Ibrahim, Caractérisation Physico-Chimique Et Minéralogique Des Argiles De La Carrière De Mirriah, Région De Zinder, Utilisées Dans La Poterie, *Eur. Sci. J. ESJ*, 17 (2021), [doi: 10.19044/esj.2021.v17n3p120](https://doi.org/10.19044/esj.2021.v17n3p120).
- [31] O. D. M. Abdoulaye, B. K. Yao, A. M. Ahmed, K. Adouby, D. M. K. Abro, P. Drogui, Mineralogical and morphological characterization of a clay from Niger, 10 (2019) 582-589.
- [32] M. Gourouza, I. Natatou, K. Bayo, A. Boos, Etude de l'adsorption d'ions fluorures par une bentonite du Niger, *J. Soc. Ouest-Afr. Chim.*, 36 (2013) 15-20
- [33] M. Thiry, N. Carrillo, C. Franke, N. Martineau, Technique de préparation des minéraux argileux en vue de l'analyse par diffraction des Rayons X et introduction à l'interprétation des

- diagrammes, Rapport Technique N° RT131010MTHI, Centre de Géosciences, Ecole des Mines de Paris, Fontainebleau, France, 34 p, (2013).
- [34] I. Mantin, R. Glaeser, Fixation des ions cobaltihexammines par les montmorillonites acides, *Bull. Groupe Fr. Argiles*, 12 (1960) 83-88, [doi: 10.3406/argil.1960.974](https://doi.org/10.3406/argil.1960.974).
- [35] A. Ksakas, K. Tanji, B. E. Bali, M. Taleb, A. Kherbeche, Removal of Cu (II) Ions from Aqueous Solution by Adsorption Using Natural Clays: Kinetic and Thermodynamic Studies, 11 (2018).
- [36] S. Barama, Développement et synthèse de deux séries de catalyseurs à base de bentonite et d'oxydes mixtes. Application à la déshydrogénation oxydante du méthane, PhD, Université Houari Boumediene, 314 (2011).
- [37] C. Bardon, Recommandations pour la détermination expérimentale de la capacité d'échange de cations des milieux argileux, *Rev. Inst. Fr. Pétrole*, 38 (1983) 621-626, [https://doi.org/doi: 10.2516/ogst:1983037](https://doi.org/10.2516/ogst:1983037).
- [38] A. A. Avidan, Chapter 1 Origin, Development and Scope of Fcc Catalysis, in *Studies in Surface Science and Catalysis*, 76 (1993), Elsevier, 1-39. [doi: 10.1016/S0167-2991\(08\)63824-0](https://doi.org/10.1016/S0167-2991(08)63824-0).
- [39] E. A. Emam, Clays as Catalysts in Petroleum Refining Industry, *ARPJ Journal of Science and Technology*, 3 (2013) 350-374.
- [40] H. Liu, T. Shen, T. Li, P. Yuan, G. Shi, X. Bao, Green synthesis of zeolites from a natural aluminosilicate mineral rectorite: Effects of thermal treatment temperature, *Appl. Clay Sci*, 90 (2014) 53-60, [doi: 10.1016/j.clay.2014.01.006](https://doi.org/10.1016/j.clay.2014.01.006).
- [41] M. A. Maman, A. Rabani, F. Habbachi, F. Menai, A. Abdoulaye, A. M'nif, Characterization of two clay minerals of the Niger River Valley: Téra and Boubon, *Journal of the Tunisian Chemical Society*, 7 (2017) 52-58.
- [42] J.-M. Avenard, J. Bonvallot, M. Latham, M. R. Dugerdil, J. Richard, Aspects du contact forêt-savane dans le centre et l'Ouest de la Côte d'Ivoire: étude descriptive, Paris : ORSTOM, (1974), 254 p. (Travaux et Documents de l'ORSTOM). ISBN 2-7099-0345-8.
- [43] A. Qlihaa, S. Dhimni, F. Melrhaka, N. Hajjaji, A. Srhiri, Caractérisation physico-chimique d'une argile Marocaine [Physico-chemical characterization of a morrocan clay], *J. Mater. Environ. Sci.* 7 (5) (2016) 1741-1750, [https://www.jmaterenvironsci.com/Document/vol7/vol7\\_N5/192-JMES-2132-Qlihaa.pdf](https://www.jmaterenvironsci.com/Document/vol7/vol7_N5/192-JMES-2132-Qlihaa.pdf)
- [44] H. S. Cerqueira, G. Caeiro, L. Costa, F. Ramôa Ribeiro, Deactivation of FCC catalysts, *J. Mol. Catal. Chem.*, 292 (2008) 1-13, [doi: 10.1016/j.molcata.2008.06.014](https://doi.org/10.1016/j.molcata.2008.06.014).
- [45] D. Munvuyi, M.S. Ousmane, M. Bougouma, Physicochemical and mineralogical characterization of clays from the Tcheriba zone in the Boucle of Mouhoun region (Burkina Faso), *J. Mater. Environ. Sci.* 13 (2022) 755-767, [https://www.jmaterenvironsci.com/Document/vol13/vol13\\_N7/JMES-2022-13062-Munvuyi.pdf](https://www.jmaterenvironsci.com/Document/vol13/vol13_N7/JMES-2022-13062-Munvuyi.pdf)
- [46] O. Bouras, Propriétés adsorbantes d'argiles pontées organophiles : synthèse et caractérisation, PhD, Université de Limoges, p.162 (2003).
- [47] P. Pialy, Etude de quelques matériaux argileux du site de Lembo (Cameroun): minéralogie, comportement au frittage et analyse des propriétés d'élasticité, PhD, Université de Limoges, p.147(2009).
- [48] B. Sorgho, P. Bressollier, B. Guel, L. Zerbo, R. Ouedraogo, M. Gomina, P. Blanchart, Étude des propriétés mécaniques des géomatériaux argileux associant la décoction de *Parkia Biglobosa* (nééré), *Comptes Rendus Chim*, 19 (2016) 895-901 [doi: 10.1016/j.crci.2016.01.016](https://doi.org/10.1016/j.crci.2016.01.016).

- [49] G. O. Ihekweze, J. N. Shondo, K. I. Orisekeh, G. M. Kalu-Uka, I. C. Nwuzor, A. P. Onwualu, Characterization of certain Nigerian clay minerals for water purification and other industrial applications, *Heliyon*, 6 (2020) 03783, [doi: 10.1016/j.heliyon.2020.e03783](https://doi.org/10.1016/j.heliyon.2020.e03783).
- [50] A. Aarfane, A. Salhi, M. El Krati, S. Tahiri, M. Monkade, E. K. Lhadi, M. Bensitel, Etude cinétique et thermodynamique de l'adsorption des colorants Red195 et Bleu de méthylène en milieu aqueux sur les cendres volantes et les mâchefers (Kinetic and thermodynamic study of the adsorption of Red195 and Methylene blue dyes on fly ash and bottom ash in aqueous medium), 13 (2014) 1927-1939.
- [51] S. Mahmoudi, A. Bennour, A. Meguebli, E. Srasra, F. Zargouni, Characterization and traditional ceramic application of clays from the Douiret region in South Tunisia, *Appl. Clay Sci.*, 127-128 (2016) 78-87, [doi: 10.1016/j.clay.2016.04.010](https://doi.org/10.1016/j.clay.2016.04.010).
- [52] H. H. Murray, Applied Clay Mineralogy: Occurrences, Processing and Applications of Kaolins, Bentonites, Palygorskitesepiolite, and Common Clays, *Elsevier*, 2006.
- [53] M. Gueye, Développement de charbon actif à partir de biomasses lignocellulosiques pour des applications dans le traitement de l'eau, PhD, Université de Limoges, p.229 (2015). <https://agritrop.cirad.fr/579887/>
- [54] A. Soualah, M. Berkani, M. Chater, Synthèse et caractérisation des zéolithes de type ZSM-5, *Comptes Rendus Chim.*, 7 (2004) 713-720, [doi: 10.1016/j.crci.2004.04.005](https://doi.org/10.1016/j.crci.2004.04.005).
- [55] M. E. kanzaoui, A. Hajjaji, A. Guenbour, R. Boussen, Development and study of mechanical behaviour reinforcing composites by waste BTP, *MATEC Web Con.*, 149 (2018) 02012, [doi: 10.1051/mateconf/201814902012](https://doi.org/10.1051/mateconf/201814902012).

(2022) ; <http://www.jmaterenvirosci.com>